Journal of Chromatography, 589 (1992) 71–85
Elsevier Science Publishers B.V., Amsterdam

CHROM. 23 701

Predictability of chromatographic protein separations

Study of size-exclusion media with narrow particle size distributions

Atul M. Athalye, Stephen J. Gibbs* and Edwin N. Lightfoot*

Department of Chemical Engineering, University of Wisconsin–Madison, 1415 Johnson Drive, Madison, WI 53706 (USA)

(First received May 1st, 1991; revised manuscript received August 23rd, 1991)

ABSTRACT

It is shown that existing models of differential chromatography are capable of predicting the behavior of polydisperse packings in commercially available columns in terms of separately determined transport and equilibrium properties. Experiments conducted using proteins on size-exclusion media with a narrow particle size distribution indicate that such packings perform as well as predicted by theory of their more expensive monodisperse counterparts. These results confirm theoretical studies and previous data suggesting that a modest degree of polydispersity has no significant effect on separation efficiency, thus allowing the direct design of large columns from basic transport and equilibrium data.

INTRODUCTION

The purpose of the work described here was to test the utility of currently available one-dimensional lumped-parameter models of differential chromatography for describing the performance of commercially available columns and packing materials. The model used for this purpose is essentially that of Gibbs and Lightfoot [1], but it differs only in detail from those of others (see, for example, the books by Giddings [2], Ruthven [3] and Jönsson [4] and the papers by Lenhoff [5] and Weber and Carr [6]). The experimental results are shown later as Van Deemter plots [7] in Figs. 3–5. Both glass (Omnifit) and stainless-steel (Alltech) columns were used in the study. The packings employed were macroporous TSK-GEL Toyopearl HW65 size-exclusion beads (TosoHaas; mean diameters 30 and 75 μm), selected for study because of their importance as support materials or base matrices that are derivatized with ion exchange, hydrophobic interaction and affinity functionalities.

Size-exclusion chromatography was chosen for this work because of its simplicity, in that the only rate parameters needed for *a priori* prediction of peak widths are intraparticle diffusivities, convective dispersion coefficients and, to a secondary degree, fluid-phase mass-transfer coefficients. As will be shown later, sufficient information of this type is available to provide a meaningful comparison between observations and *a priori* predictions of plate heights. On the other hand, accurate estimates of geometric and thermodynamic parameters (collectively called equilibrium parameters) such as the inclusion porosity of a species, which determine the peak position in the differential mode of operation,

* Present address: University of Cambridge School of Clinical Medicine, Herchel Smith Laboratory for Medicinal Chemistry, University Forvie Site, Robinson Way, Cambridge CB2 2PZ, UK.

0021-9673/92/$05.00

are best obtained directly from experiment, and no attempt is made here to predict them.

Our interest centered on two specific practical questions: (i) are existing lumped-parameter models adequate to describe the behavior of commercially available chromatographic media?, and (ii) is monodispersity of the packing material necessary to achieve maximum separation efficiency?

Before turning to our results and their significance, we summarize the model used for differential chromatography, then briefly review the pertinent literature in the context of the model and outline our experimental procedure.

CHROMATOGRAPHIC MODEL

We deal here with linear chromatography in which the equilibrium constant for adsorption and the fluid properties are considered to be independent of concentration, a reasonable assumption for dilute samples or low loadings. The model is formulated for an adsorptive system, with size-exclusion chromatography treated as a special case. The details of the problem statement are given in the Appendix in order to clarify our notation, which differs slightly from that of Gibbs and Lightfoot [1]. In this section, we first present a solution to the model equations valid for long columns, then provide an overview of available information on the transport parameters which appear in the model and finally discuss the issue of predictability of chromatographic performance.

Asymptotic long-time solution

Some of the earliest solutions of the pseudo-continuum equations of linear chromatography for specific cases of the dominant broadening mechanisms were obtained by, among others, Lapidus and Amundson [8] and Rosen [9]. Rasmuson [10] later derived a general solution which includes the effects of convective axial dispersion, fluid-phase mass transfer, intraparticle diffusion and linear adsorption kinetics. The expression being tested here is a convenient lumped-parameter approximation to these solutions, developed by Reis *et al.* [11] for rapid adsorption and extended by Gibbs and Lightfoot [1] to include the effects of adsorption kinetics and to treat gradient elution. It has been shown that this solution combines simplicity with a surprising degree of accuracy and that it should be adequate for most purposes in liquid chromatography [1,5].

Differential chromatography involves the application of a short feed pulse into the mobile phase of a column previously devoid of solute. The initial conditions for the concentrations in the fluid and stationary phases can then be written as

$$c_f(z,t=0) = \frac{m_0}{A_0\varepsilon_b}\delta(z) \quad \text{and} \quad c_b(z,t=0) = 0 \tag{1}$$

respectively, where A_0 is the column cross-sectional area, m_0 is the mass (or moles) of solute initially injected, ε_b is the interstitial void fraction and $\delta(\cdot)$ is the Dirac delta function. Columns of interest for practical separations are typically long in the sense that the boundary conditions have little effect on the peak shape [5]. It is hence convenient to use the simplest type of physically reasonable boundary conditions, and here we choose the long-column form, which assumes that the concentration field decays rapidly at long distances:

$$\lim_{z\to\pm\infty} c_f = \lim_{z\to\pm\infty} c_b = 0 \tag{2}$$

In order to test the utility of the model, we need only consider isocratic operation, in which case the long-time solution to the equations of linear chromatography is a Gaussian function [11] of the axial coordinate z in the column:

$$c_f(z,t) = \frac{m_0 u}{A_0\varepsilon_b\sqrt{2\pi H z_0}}\exp\left[\frac{-(z-z_0)^2}{2Hz_0}\right] \tag{3}$$

with

$$z_0 \equiv uvt \quad \text{and} \quad u \equiv \frac{\varepsilon_b}{\varepsilon_b + (1-\varepsilon_b)\varepsilon_p^*(1+K_d)} \tag{4}$$

where v is the interstitial fluid velocity and the quantity u represents the fraction of solute in the moving fluid phase at long times. Here K_d is the equilibrium constant for adsorption, defined as the ratio of the mass of adsorbed solute to that of unadsorbed solute *within a particle* at equilibrium, while ε_p^* is a species-dependent inclusion porosity which represents the fractional volume of stationary phase that is effectively accessible to a solute. (We note as an aside that a simplification results for size-exclusion chromatography, where $K_d = 0$).

Both the variance and mean of the Gaussian function in eqn. 3 vary linearly in time and hence their ratio H, the height equivalent to a theoretical plate (HETP or plate height) [12], is a useful time-independent measure of column performance. It follows that a small plate height implies a relatively narrow peak, and hence better separation performance. Note that solutions for other initial conditions can be written in terms of the Gaussian expression above by means of a superposition [13].

The present description of linear chromatography allows us to express the plate height in terms of the lumped parameters which characterize the different mechanisms of peak broadening in a packed bed [1,5,11]. It is instructive and convenient to write the explicit expression for plate height in dimensionless terms by defining a reduced plate height, $h \equiv H/2R$. We then have the following extension of the Van Deemter equation [7]:

$$h = \frac{2}{Pe_{\mathscr{E}}} + \frac{(1-u)^2}{3(1-\varepsilon_b)}(ReSc)\left[\frac{1}{Nu} + \frac{m}{10} + \frac{m'}{Da}\right] \quad (5)$$

Here the dispersion Péclet number $Pe_{\mathscr{E}}$ and the Nusselt number Nu are simply scaled representations of the convective axial dispersion coefficient $\mathscr{E}$ and the fluid-phase mass-transfer coefficient k_c, as defined below:

$$Pe_{\mathscr{E}} \equiv \frac{2Rv}{\mathscr{E}} \quad \text{and} \quad Nu \equiv \frac{2Rk_c}{\mathscr{D}_f} \quad (6)$$

Both these dimensionless numbers are functions of the interstitial void fraction ε_b and the reduced velocity $ReSc \equiv 2Rv\varepsilon_b/\mathscr{D}_f$, as discussed later. The typical velocity range of interest in liquid chromatographic practice is $1 < ReSc < 200$, with size-exclusion chromatography usually conducted below $ReSc = 50$. The terms involving the quantities m and m', defined as

$$m \equiv \frac{\mathscr{D}_f}{\varepsilon_p^* \mathscr{D}_p} \quad \text{and} \quad m' \equiv \frac{3}{2}m\left(\frac{K_d}{1+K_d}\right)^2 \quad (7)$$

are respectively the contributions of the intraparticle diffusion resistance and sorption kinetics to peak broadening; the Damköhler number $Da \equiv R^2 k_a/\mathscr{D}_p$.

We shall henceforth be concerned with size-exclusion chromatography, where K_d and m' vanish, so that the term involving Da in eqn. 5 will not be needed any further in our discussion. The reduced plate height is commonly displayed as a function of the dimensionless velocity $ReSc$ in a Van Deemter plot [7] which, it may be observed, does not depend explicitly on particle size.

Description of transport parameters

In this section, we provide information available in the literature on the three transport parameters needed to characterize the performance of size-exclusion chromatography, namely, the intraparticle diffusivity, the convective dispersion coefficient and the fluid-phase mass-transfer coefficient.

We begin by noting that at the low concentrations encountered in linear chromatography, the diffusivity of a solute can be assumed to be independent of concentration, as done in the analysis above. It is also adequate to follow the commonly used practice of considering the intraparticle diffusivity to be proportional to that in free solution, with the proportionality constant depending on the size of the pores relative to that of the solute and on the shape and tortuosity of the pores [14]. Expressions for this proportionality constant, derived from a simplified hydrodynamic model of pore-wall effects and written in terms of the solute-to-pore size ratio, have been used successfully in the literature [14–16] for both correlative and predictive purposes. However, our particular experimental system allows us to proceed without this detailed information, a point we shall pursue further in the section on plate-height predictions.

We now present what we consider to be the most reliable correlations available in the literature for the lumped parameters $Pe_{\mathscr{E}}$ and Nu defined above. It is known from the continuum form of the equations of change [17] that for transport in forced convective flow, the scaled state variables of a system, and hence dimensionless quantities derived from them (such as $Pe_{\mathscr{E}}$ and Nu), depend parametrically on system geometry and the Reynolds and Schmidt numbers, given respectively as

$$Re \equiv \frac{2Rv\varepsilon_b\rho}{\mu} \quad \text{and} \quad Sc \equiv \frac{\mu}{\rho\mathscr{D}_f} \quad (8)$$

where ρ and μ are the density and viscosity of the fluid. It turns out that modern liquid chromatography is almost always conducted in the creeping flow regime, defined for packed beds by the Reynolds number being of the order of unity or

smaller. This fact is of significance because creeping flow is qualitatively different in nature from high-*Re* flow (of which turbulent flow is a special case), owing to the dominance of viscous effects over inertial effects at low Reynolds numbers. Under these conditions, it can be shown on purely dimensional grounds [17] that the dimensionless transport coefficients should depend on *Re* and *Sc* only through their product, the reduced velocity *ReSc*, which is also called the diffusion Péclet number. The correlations given below satisfy this requirement. Moreover, experience suggests that the most important determinant of the flow geometry in a well-packed, random bed of spheres is the interstitial void fraction ε_b. It is hence customary to express the dimensionless transport parameters as functions of *ReSc* and ε_b in creeping flow.

We proceed first to an overview of available information on convective dispersion coefficients, and we begin by examining behavior under limiting conditions. Several investigations [18,19] have confirmed that for $ReSc \ll 1$, the dispersion coefficient is simply $\mathscr{D}_f/\tau$, indicating purely diffusive axial spreading; here τ is the interstitial tortuosity factor, about 1.4 for a packed bed of spheres (for simplicity, however, we retain the term "convective dispersion" even in this diffusion-dominated regime). On the other hand, for very high *ReSc* values, the dispersion Péclet number approaches an asymptotic value which depends only on the Reynolds number [20–22], corresponding to the limit of purely hydrodynamic dispersion [23]. Gunn [24] has correlated this high-*ReSc* limit in the form

$$Pe_{\mathscr{g}} \approx \frac{2p}{(1-p)} \quad \text{for very high } ReSc \tag{9}$$

where the adjustable parameter p for a column packed with spheres is found from experiment to be

$$p \equiv 0.17 + 0.33\exp(-24/Re) \tag{10}$$

Thus p is constant at 0.17 in creeping flow, giving a limiting $Pe_{\mathscr{g}}$ of about 0.4.

The behavior for intermediate values of reduced velocity has been analyzed by several workers [2,24,25]. Of these, Gunn [24,26] has carried out a semi-theoretical treatment which involves the adjustable parameter p given above, leading to the development of a correlation capable of predicting convective axial dispersion coefficients reasonably well over a wide range of conditions for both gases and liquids:

$$\frac{1}{Pe_{\mathscr{g}}} = \frac{(1-p)}{p}\left[Y + Y^2\left(\exp(-1/Y) - 1\right)\right] + \frac{\varepsilon_b}{\tau ReSc} \tag{11}$$

where

$$Y \equiv \frac{p(1-p)ReSc}{4\alpha_1^2(1-\varepsilon_b)} \tag{12}$$

Here α_1 is the smallest positive zero of the Bessel function $J_0(\cdot)$ and is approximately 2.405, p is given by eqn. 10 and τ is as mentioned above. It is easy to see that this expression for $Pe_{\mathscr{g}}$ depends only on the product *ReSc* when attention is restricted to creeping flow (with $p = 0.17$) and that it reduces to the widely accepted asymptotic results quoted in the preceding paragraph. Gunn [26] has also provided an extension of the above correlation to account for macroscopically non-uniform flow and wall effects.

It should be emphasized that no empirical correlation is perfect, especially when the objective of the correlation is to fit data over a wide range of variables, and caution is recommended in the use of such results. For example, large discrepancies are seen between Gunn's correlation and the dispersion coefficients measured by Miller and King [22] for reduced velocities between 7 and 50 in creeping flow. We hence seek a description which provides a reasonable upper bound on dispersion coefficients (or a lower bound on $Pe_{\mathscr{g}}$) for intermediate *ReSc* values in creeping flow.

Among data available in the literature [27,28] for the creeping flow regime are those of Rifai *et al.* [29], Hiby [23], Miller and King [22], Knox and Parcher [30] and Han *et al.* [28]. Some of this work does not appear to be reliable, either because narrow columns were used [30] or because the methods of analysis seem to have introduced large errors in the measured dispersion coefficients [29]. Also, the data sets of Han *et al.* and Hiby do not exhibit the limiting behavior at high *ReSc* observed by others, as will be seen shortly.

We therefore considered the data of Miller and King for obtaining a conservative upper estimate for the convective dispersion coefficient. The data points chosen for an empirical fit over intermediate reduced velocities ($7 < ReSc < 320$) and for $Re <$

1 correspond to eight runs (tabulated and numbered 12–16, 22, 24 and 25 in ref. 31) which show the most reproducibility in repeated experiments. The coordinates chosen for the fit, displayed in Fig. 1, are those suggested by Gunn's expression, namely $Pe_{\mathscr{E}}$ and $ReSc/(1-\varepsilon_b)$, and the following result then summarizes the data of Miller and King:

$$Pe_{\mathscr{E}} = \left(\frac{ReSc}{1-\varepsilon_b}\right)^{-1/6} \tag{13}$$

Also shown in Fig. 1 for comparison are the predictions of Gunn's correlation, the fit for the data of Han *et al.* (Fig. 9 or 15 in ref. 28) and the correlation given by Hiby. The fit from Han *et al.* for $10^2 < ReSc/(1-\varepsilon_b) < 10^3$ is given by

$$Pe_{\mathscr{E}} = 4.36\left(\frac{ReSc}{1-\varepsilon_b}\right)^{-0.262} \tag{14}$$

and Hiby's correlation [23] is

$$\frac{1}{Pe_{\mathscr{E}}} = \frac{0.65}{1.0 + 7.0\sqrt{\varepsilon_b/ReSc}} + \frac{0.67\varepsilon_b}{ReSc} \tag{15}$$

As seen in Fig. 1, the discrepancy between the fit to the Miller and King data and Gunn's predictions becomes markedly small towards high *ReSc*. However, the other two curves, corresponding to eqns. 14 and 15, are seen to predict dispersion coefficients much less than the first two. The discrepancies observed in Fig. 1 elude explanation, and we shall return to this point in the discussion of our results. We stress that eqn. 13 is not to be interpreted as any more than a convenient analytical representation of one particular data set. The comparison in Fig. 1, however, serves to underscore the existing uncertainty in the estimation of convective dispersion over the intermediate range of reduced velocities. It is generally believed that the typical behavior, if such a notion makes sense for convective dispersion in packed beds, probably lies between the limits given by the expression of Gunn and the data of Miller and King ($Pe_{\mathscr{E}}$ between 0.5 and 1.0 over the range of interest [32,33]). In any case, it is clear that more work is necessary to rectify the dearth of reliable data and thus obtain a better understanding of convective dispersion in granular beds.

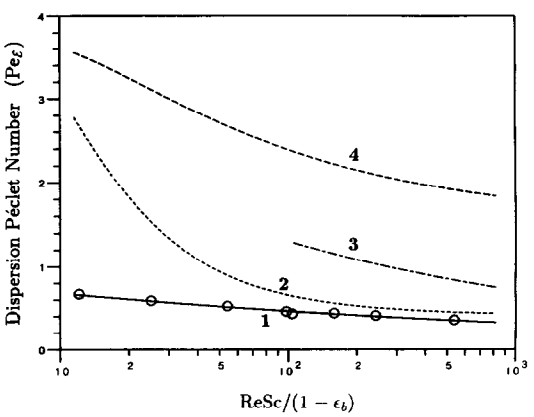

Fig. 1. Comparison of dispersion Péclet numbers ($Pe_{\mathscr{E}} \equiv 2Rv/\mathscr{E}$) from various sources. The data points are those of Miller and King (see text) and the solid line (curve 1) is the fit given by eqn. 13; curve 2 depicts the correlation of Gunn (eqn. 11); curve 3 shows the fit from the work of Han *et al.* (eqn. 14); and curve 4 is the correlation of Hiby (eqn. 15) with $\varepsilon_b = 0.4$.

On the theoretical side, Koch and Brady [34] have carried out an asymptotic analysis of dispersion, valid for low volume fractions of randomly configured spheres held fixed in a creeping ambient flow. Their prediction of the convective axial dispersion coefficient, derived for $ReSc \gg 1$, does capture the general trend of the experimental measurements taken from the literature, but severely underestimates the data over *ReSc* values between 1 and 200. (For the sake of completeness, we mention that the diffusion Péclet number in the original expression of Koch and Brady has been erroneously transcribed elsewhere in the literature [6,35].)

We hence restrict ourselves to the use of eqn. 11 and 13 as two representative limits of convective dispersion for predictive purposes later.

Having discussed the available information on convective axial dispersion, we turn now to transport between the mobile fluid far from a spherical particle and the fluid at the particle surface. As noted earlier, the fluid-phase mass-transfer coefficient k_c which characterizes the mass flux at the particle surface can be expressed in terms of a Nusselt number *Nu*. Boundary-layer theory predicts the asymptotic functional dependence of *Nu* for large values of *ReSc* [36] in creeping flow to be of the form

$$Nu = \gamma(ReSc)^{1/3} \quad (\text{for } ReSc \gg 1) \tag{16}$$

Wilson and Geankoplis [37] found their measurements from electrochemical experiments to follow this dependence fairly accurately, and obtained γ =

$1.09/\varepsilon_b$. As far as the behavior at low values of *ReSc* is concerned, there appears to have been some uncertainty in the literature [38], but both analysis [39,40] and experiment [41,42] suggest that the Nusselt number approaches a constant value β as $ReSc \to 0$, much as with an isolated sphere in a stagnant fluid [17].

Following the procedure employed in ref. 43 for patching up asymptotic results, we used this limiting information to develop the following expression:

$$Nu \approx [\beta^3 + \gamma^3(ReSc)]^{1/3} \tag{17}$$

where γ is as above and β is conservatively chosen [39] to be 4.0. This cube-averaged form has been selected because it conforms to the limiting behavior mentioned above and gives uniformly good agreement (within 10%) with the numerical results of Sørensen and Stewart [39] over five decades of *ReSc*. It can be shown that the large *ReSc* limit is adequate for most practical purposes because the contribution of fluid-phase mass-transfer resistance to plate height is negligibly small at low *ReSc*, so that the plate height is not particularly sensitive to the choice of β.

This completes the description of the chromatographic model used in this study.

Predictability of chromatographic performance

At this juncture, it is worth pointing out that a number of empirical relationships for the dependence of the reduced plate height have emerged in the literature. Perhaps the most successful of these is the so-called Knox equation [44,45], given here in a general form:

$$h = A(ReSc)^{1/3} + \frac{B}{ReSc} + CReSc + D \tag{18}$$

where A, B, C and D are empirical constants for a given column, eluent and solute. This equation, however, may not be very useful for process design when extrapolating from laboratory conditions, inasmuch as the empirical constants here are not directly related to independently measurable quantities such as those in eqn. 5. Although the C-term above, for example, can be related to an effective stationary-phase diffusion coefficient [46], it is desirable for design purposes to retain a distinction between the individual contributions, as done in eqn. 5. Weber and Carr [6] have reviewed the origins and validity of eqn. 18 and its competitors.

We now consider the issue of predictability of chromatographic separations using the lumped-parameter model outlined in the preceding sections. We shall shortly see that the Gaussian solution and the plate-height expression given above yield accurate descriptions of (linear and isocratic) size-exclusion chromatography in the differential mode, *given reliable values of the transport parameters involved.* The correlations for convective axial dispersion and fluid-phase mass transfer quoted from the literature are adequate for most purposes, except at low reduced velocities where convective dispersion is poorly understood. However, in order to use the above model for design predictions, transport parameters such as the factor m (which involves the intraparticle diffusivity) in eqn. 5 must still be obtained by other means, because these parameters cannot be determined reliably using the plate-height equation as a basis for analyzing experimental data [5,47].

Such a situation is not unusual in engineering practice, and a simple example in point concerns the extraction of intraparticle diffusion coefficients from the plate height measured in a single size-exclusion experiment at a relatively low velocity and its use for predicting chromatographic behavior at high velocities. At low velocities, convective axial dispersion dominates the plate height, but the considerable uncertainty in its prediction (as indicated in the previous section) can lead to an uncertainty in the value of intraparticle diffusivity extracted. As a result, the plate height predicted at high velocities, where intraparticle diffusion is the dominant resistance, on the basis of the low-velocity data would likely be in error by a significant amount. Another illustration is afforded by the work of Nakanishi *et al.* [48] on size-exclusion chromatography. They found that the diffusivity ratio calculated from the slope of the measured Van Deemter plot was about half of that determined from experiments conducted on single gel beads, suggesting that there was significant bypassing or channelling in the columns used.

We have therefore concentrated in our program on reliable means for estimating the parameters appearing in the above description in isolation from each other, using separate, well-defined experiments

[35,49]. Some of our results to date are used later in this study.

Before moving to a description of our experiments and predictions, we briefly summarize prior work published in the literature on the effect of polydispersity of packing material on performance.

PRIOR WORK ON THE EFFECT OF POLYDISPERSITY

In this section, we review the effect of particle size distribution (PSD) on three interrelated factors: the plate height or separation performance, the packing quality and the pressure drop in a fixed bed.

The effect of polydispersity of packing media on chromatographic performance has been studied experimentally by only a few investigators. Dawkins *et al.* [50] published one of the early studies on PSD in gel permeation chromatography using cross-linked polystyrene gels, but for the most part only compared distributions with different mean sizes. A careful examination of their data reveals, however, that for a completely excluded solute, the plate heights of narrowly distributed and monodisperse media (with the same mean size) were similar. Moreover, the observed limiting behaviour of the plate height for high values of the dimensionless group *ReSc* appears to be consistent with the prediction from Gunn's correlation for the convective dispersion coefficient (eqn. 11).

Later, Nakanishi *et al.* [48], in a series of papers on dispersion mechanisms in size-exclusion chromatography, investigated the performance of Sephadex (Pharmacia) gels, with sodium chloride and myoglobin as solutes. They found that for each solute, the dimensionless Van Deemter plots for different sieve fractions did collapse into a single line as expected from eqn. 5, but only when the particle size used for scaling was chosen as the volume-averaged root-mean-square diameter calculated from the PSD of each sieve fraction. From eqn. 5, this result is seen to be consistent with the intraparticle diffusion resistance dominating the plate height.

Most recently, Han *et al.* [28] studied two sets of non-porous particles with a discrete distribution of sizes and compared their convective dispersion coefficients with those obtained from monodisperse beads, with all three sets having the same area-averaged mean particle diameter. It was observed that the narrower distribution and the uniform set behaved almost identically, whereas the particles which were broadly distributed gave dispersion coefficients higher by a factor of two.

As far as theoretical analyses on this topic are concerned, a few workers have carried out numerical solutions of special cases of the equations of change to investigate the effect of PSD on performance in chromatography [51–55] and in stirred batch systems [56]. The general consensus from all these investigations is that polydispersity may have an adverse impact on the broadening of a peak or a front only for very broad or asymmetric PSD in a short bed. For columns with the large number of plates typically necessary for protein separations, it appears adequate to use chromatographic media with a symmetric size distribution of modest breadth. This conclusion also seems to imply that the use of a mean diameter is reasonable for design calculations under the conditions noted above, an important point we shall use in our predictions.

We next come to the issue of packing quality in relation to polydispersity. The most recent experimental work on this subject is that of Kulin *et al.* [57], who prepared remarkably monosized poly (styrene–divinylbenzene) particles of 5, 10 and 20 μm diameter for size-exclusion chromatography. They encountered a lack of reproducibility in experiments on columns packed with 5-μm beads, and found that two identically sized columns with 10- and 20-μm particles had interstitial voidages as high as 0.58 and 0.47, respectively. These observations cast doubts on the reliability of the slurry packing method used and on the resulting packing quality using such monodisperse media, and preclude any definitive conclusions on this topic.

The last consideration regarding PSD is its effect on the pressure drop in a packed bed, and two representative studies are cited here. Dewaele and Verzele [58] worked with silica-based reversed-phase sorbent materials (Alltech) made as mixtures of two narrowly distributed fractions and showed that the pressure drop in columns packed with mixtures of very different size fractions was well above that predicted by using the arithmetic mean diameter in the Blake–Kozeny equation [17]. In contrast, Yamamoto *et al.* [59] found that the Blake–Kozeny equation was satisfactory for their columns packed with Toyopearl HW55 media (TosoHaas), which have a reasonably narrow size distribution.

Having discussed the reported effects of polydispersity on chromatography, we now proceed to a description of the experimental work undertaken.

EXPERIMENTAL OBSERVATIONS

As a part of the larger goal of separately measuring transport parameters and using these estimates for the design and scale-up of chromatographic separations, the work described in this section involved the use of size-exclusion column experiments for assessing the general performance of the Toyopearl HW65 media.

Experiments on differential chromatography were conducted on two sets of columns. (i) One set consisted of two glass columns (Omnifit) with the same I.D.(2.50 cm) and bed lengths of 11.5 and 46.5 cm (chosen so as to study the dispersion from column ancillaries). This pair of columns was packed at TosoHaas by the constant-pressure method at 2 bar with a 30% slurry of the vinyl polymer-based, macroporous size-exclusion medium Toyopearl HW65C, which has a particle size range of 50–100 μm. (ii) The other consisted of a 25.0 $\times$ 2.25 cm I.D. stainless-steel column (Alltech) packed with Toyopearl HW65S, nominally the same medium as above, but with a size range of 20–40 μm. This column was packed by adding a slurry of the gel particles under gravity-induced flow. The bed was then allowed to settle under a flow of 5 ml/min. Finally, a small amount of additional packing was added to fill voids at the top of the column resulting from the settling.

For the glass columns, injections of *ca.* 0.1 ml of bovine hemoglobin (Sigma; No. H 2500) at concentrations of 10, 50 and 100 mg/ml were applied, whereas for the stainless-steel column, the samples were 20 mg/ml ovalbumin (Sigma; No. A 5503) in volumes of about 0.02 ml for the first set of data and 0.1 ml for data taken 2 months later. In all instances, the samples were made up in 0.1 *M* Tris–HCl buffer (pH 8) and applied using a Rheodyne (Model 7125) valve. The pulse response experiments were run at a series of flow-rates with elution by the above buffer, filtered and degassed, using Gilson Model 303 pumps. The column effluent concentration was monitored by measuring the UV absorption at 254 or 280 nm across 2- or 10-mm flow cells for hemoglobin and at 280 nm across a 10-mm flow cell for ovalbumin, both in a Gilson Holochrome detector (cell volumes under 11 μl). The output was acquired digitally and stored using a PDP 11/75 computer (Digital Equipment). All the work described here was carried out at room temperature (20°C).

Two preliminary experiments were conducted to measure the interstitial void volume in the columns and to quantify the effects of extracolumn fittings including the injection valve, tubing and detector on measured effluent chromatograms. For the former experiment, both blue dextran (Sigma; No. D 5751) and calf thymus DNA (Calbiochem) [60] were used individually, but were found to have broad molecular weight distributions. For the short glass column, the least retained component of blue dextran, which was isolated and eluted separately, repeatedly indicated an interstitial void fraction of about 0.36, as did the runs with DNA, whereas DNA elution on the long glass column suggested a voidage close to 0.39. For the stainless-steel column, experiments with DNA gave a void fraction of about 0.31. The other set of preliminary runs for studying the additional dispersion from extra-column fittings consisted of disconnecting the columns from the flow path and carrying out pulse response measurements. It was determined that these contributions to the broadening of a pulse sent to the column were negligible enough to cause less than a 1% change in the plate height of the shortest column used here even when operated at its most efficient.

The elution curve for each run was fitted to the long-column Gaussian solution (eqn. 3 with z held constant at the column length) by a non-linear least-squares fitting routine developed at the University of Wisconsin [61]. We eschewed the use of methods based on tangents or moments or on information derived from isolated points on the chromatogram, as these procedures are generally unreliable or prone to numerical errors [5]. A sample chromatogram with the best fit is shown in Fig. 2. As the peak in each experiment was digitally sampled in a set of 150–300 points, the fitting code provided confidence limits of better than 3% on the three parameters estimated *in each run*, namely, the inclusion porosity, the plate height and a measure of the mass of solute injected. (The solute mass was left as a quantity to be estimated because the injection volumes and sample concentrations were not con-

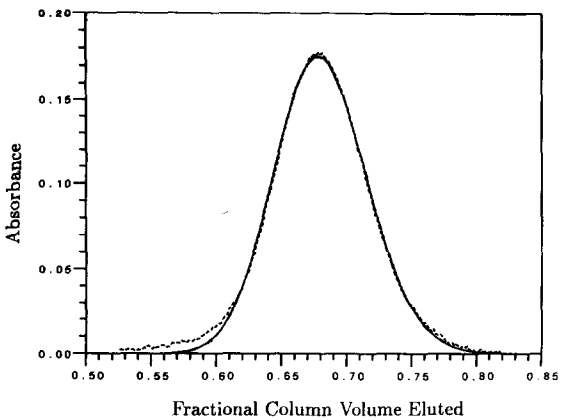

Fig. 2. Comparison of an effluent chromatogram shape with a least-squares best fit (solid line) based on the Gaussian expression in eqn. 3. A 0.1-ml sample of 10 mg/ml hemoglobin was eluted at 0.6 ml/min in an 11.5 × 2.5 cm I.D. glass column packed with Toyopearl HW65C; absorbance was measured at 280 nm across a 10-mm path length. Parameter values estimated: $\varepsilon_p = 0.498$ and $h = 4.16$. The number of data points on the digitized chromatogram used for fitting was 246 in this instance. Other details are given in the text.

trolled to the same degree of accuracy as reflected in the confidence limits given by the fitting routine; from eqn. 3 it is clear that doing so should not affect the estimation of the other two parameters.)

The estimates obtained for the inclusion porosity ε_p^* were as follows: a mean value of 0.503 for hemoglobin in HW65C in the 11.5-cm glass column, based on 39 separate runs over a range of flow-rates [relative standard deviation (R.S.D.), 1.4% of the mean]; 0.491 for hemoglobin in HW65C in the 46.5-cm glass column, based on 19 runs (R.S.D., 1.2%); and 0.454 for ovalbumin in HW65S in the stainless-steel column, based on 17 runs (R.S.D., 1.9%). The value for ovalbumin in HW65S is consistent with that measured by Germershausen *et al.* [60] in Toyopearl HW65F (size range 30–60 μm). Also, the values of ε_p^* for hemoglobin in HW65C are seen to agree fairly closely with each other when measured on two columns of different length. However, this value for hemoglobin (molecular weight 64 kilodalton) in HW65C is larger than that for the slightly smaller protein ovalbumin (45 kilodalton) by about 10%, with the latter porosity measured in HW65S, which is putatively the same medium as HW65C but has a different particle size. In a macroporous gel such as HW65 with a reported protein exclusion limit of 5 megadalton [62], these two molecules are expected to have roughly the same degree of partition, and the discrepancy of 10% is then not practically significant for this medium.

This observation suggests to us that our measurements of interstitial voidage are probably not completely accurate. Indeed, from the form of eqn. 4, it is clear that the parameter ε_p^* in size-exclusion chromatography is very sensitive to ε_b and the elution volume, so that small errors in the measurement of the solute mean residence time and void fraction can become magnified into large errors in the estimates of the inclusion porosity. As an illustration of this sensitivity and the concomitant tendency for error in parameter estimation, we point out that Yamamoto *et al.* [63] and Germershausen *et al.* [60] obtained results that give inclusion porosities differing by 20–25% *for a given protein in the same medium.* These two groups worked with Toyopearl HW55F, each using both ovalbumin and bovine serum albumin (69 kilodalton), but with different buffers (Tris–HCl and KCl–phosphate, respectively).

We shall return to the effect of the small uncertainty in the estimation of the inclusion porosity briefly in the next section. To summarize, we obtained an average inclusion porosity of the medium in each column for the respective proteins, and also measured values of plate height as a function of velocity for different samples sizes and concentrations. The maximum interstitial velocities used in this study were 1.6 and 1.1 cm/min for the short and long glass columns, respectively, and 4.0 cm/min for the stainless-steel column, corresponding to a range of *ReSc* values between 0.7 and 110. Our data therefore covered the normal velocity range of operation of size-exclusion columns, namely 0.5–1.5 cm/min.

PLATE-HEIGHT PREDICTIONS

Our goal now is to calculate the plate height as a function of interstitial velocity essentially *a priori*, using only the values of void fraction and inclusion porosity determined from experiment. The two major hurdles in this approach are the lack of knowledge of the intraparticle diffusivity and of a mean particle size for use in the reduced plate-height equation given previously.

As mentioned earlier, it is convenient and ade-

quate to assume that the intraparticle diffusivity of a solute is proportional to its free-solution diffusivity, with the effective tortuosity factor $\mathscr{D}_f/\mathscr{D}_p$ dependent on the relative sizes of the solute and the pores. Gibbs and co-workers [64,65] measured ovalbumin diffusivities by pulsed field gradient NMR in solution and inside Toyopearl HW65 media at 20°C and found that the ratio $\mathscr{D}_f/\mathscr{D}_p$ is between 2.2 and 2.4 over the concentration range 1–200 mg/ml. This effective tortuosity factor can be expected to apply also to hemoglobin, inasmuch as the hemoglobin and ovalbumin molecules are comparable in size (radii of gyration 25 and 22 Å, respectively [66]) and both much smaller than the pores of the HW65 media (protein exclusion limit 5 megadalton) [62]. We hence do not need explicitly to use any predictive expression for the pore-wall effect [14], as indicated in the section on the description of transport parameters. The free-solution diffusivity of hemoglobin at 20°C is available in the literature [66,67]. For the purposes of prediction, it was assumed that the intraparticle diffusivity for hemoglobin differs from the free-solution value simply by a factor of about 2.3 for the HW65 media. As an aside, we mention that the slope of the plate-height data of Yamamoto *et al.* [63] yields a high diffusivity ratio of about 7.0 for myoglobin (16 kilodalton) in the Toyopearl HW55 media, which have an exclusion limit of 700 kilodalton and pores presumably narrower than those of HW65.

A study of the particle size distribution of the HW65 media (conducted at Rohm and Haas Research Labs. using a Malvern laser light-scattering device) indicates that the bead diameters are narrowly distributed about the arithmetic mean of the upper and lower size limits quoted by the manufacturer, with a d_{90}/d_{10} ratio of only 1.2 (d_{90} and d_{10} refer to the sizes below which 90% and 10% of the particles are found). Moreover, the number-, area- and volume-averaged particle diameters are found to be close to the arithmetic mean size. Then, in accordance with the discussion of prior work on the effect of polydispersity, it appears reasonable to use the arithmetic mean particle diameter for both the size fractions used here.

The system properties assumed for predicting plate heights from eqn. 5 are summarized in Table I. From information available in the original sources cited, the diffusivity values shown are considered accurate to about 10% or better. The predictions for the convective dispersion coefficients were made using Gunn's semi-empirical correlation (eqn. 11) and the Miller and King fit (eqn. 13) (although the latter is based on data for $ReSc > 7$, we have used it down to $ReSc = 2$ for clarity). The mobile phase mass-transfer coefficient was obtained using eqn. 17. The predictions are accurate to about 5% on the basis of the diffusivity values used. Finally, we mention that the calculated plate-height curves were found to be insensitive to variations of 10% in the value of the inclusion porosity, which corresponds to the extent of discrepancy in our observations mentioned in the previous section.

RESULTS AND DISCUSSION

The observations and predictions of plate height in size-exclusion chromatography are compared in Figs. 3, 4 and 5 for the three columns used with the two proteins and the two particle sizes noted above. As expected for the small loadings used here, the plate height is not particularly sensitive to the injected solute concentration in the case of the professionally packed glass columns. With the stain-

TABLE I

PARAMETER VALUES USED FOR PLATE-HEIGHT PREDICTIONS IN FIGS. 3–5

Parameter	Fig. 3	Fig. 4	Fig. 5
Particle radius (R, μm)	37.5	37.5	15.0
Solution diffusivity ($\mathscr{D}_f$, cm^2/s)	$6.9 \cdot 10^{-7}$	$6.9 \cdot 10^{-7}$	$7.9 \cdot 10^{-7}$
Pore diffusivity ($\mathscr{D}_p$, cm^2/s)	$3.0 \cdot 10^{-7}$	$3.0 \cdot 10^{-7}$	$3.3 \cdot 10^{-7}$
Bed void fraction (ε_b)	0.36	0.39	0.31
Inclusion porosity (ε_p^*)	0.503	0.491	0.454

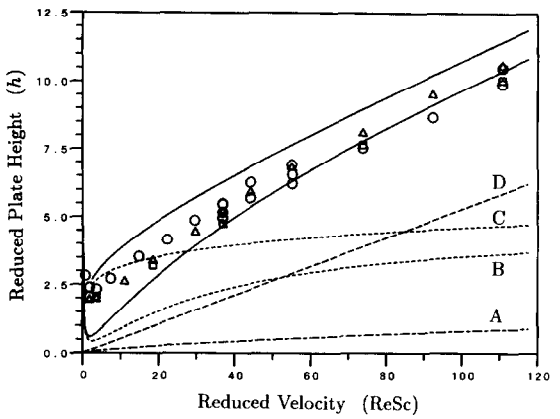

Fig. 3. Plate-height data for an 11.5 × 2.5 cm I.D. glass column packed with Toyopearl HW65C obtained from the elution of 0.1-ml bovine hemoglobin samples with concentrations of (○) 10, (△) 50 and (□) 100 mg/ml. The contributions to the reduced plate height from individual broadening mechanisms, predicted by means of eqn. 5 and the parameter values in Table I, are as follows: (A) mobile phase mass-transfer term (eqn. 17); (B) axial dispersion prediction using Gunn's correlation (eqn. 11); (C) axial dispersion prediction from the Miller and King fit (eqn. 13); and (D) intraparticle diffusion resistance. The lower and upper solid lines represent the total reduced plate height based on curves B and C, respectively. Note that an *ReSc* value of 100 corresponds to a velocity of about 1.5 cm/min.

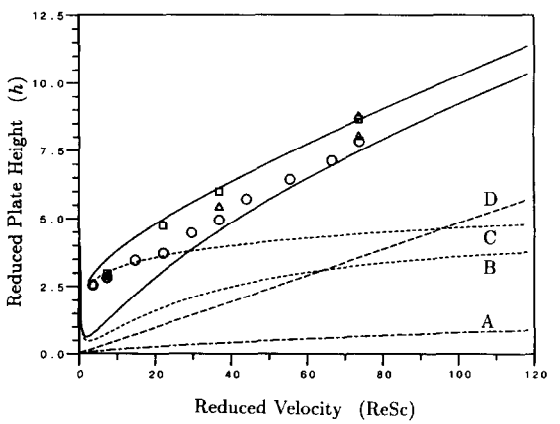

Fig. 4. Plate-height data for a 46.5 × 2.5 cm I.D. glass column packed with Toyopearl HW65C obtained from the elution of 0.1-ml bovine hemoglobin samples with concentrations of (○) 10, (△) 50 and (□) 100 mg/ml. The predictions of plate height and the break-up into its constituent contributions are as in Fig. 3. To allow comparison between the long and short columns, the scale used is as in Fig. 3. Note that an *ReSc* value of 100 corresponds to a velocity of about 1.4 cm/min.

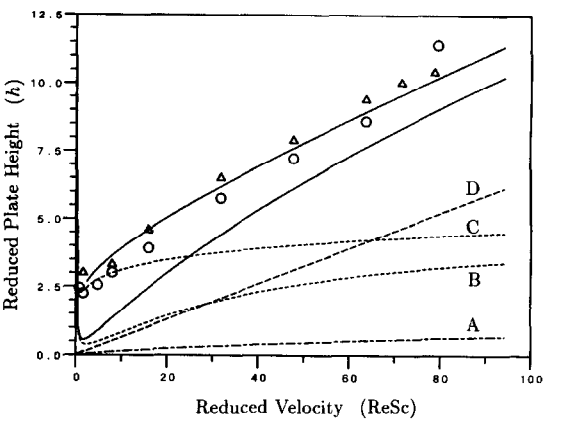

Fig. 5. Plate-height data for the 25.0 × 2.25 cm I.D. stainless-steel column packed with Toyopearl HW65S, obtained from the elution of 20 mg/ml ovalbumin samples. Injected volumes were (○) 0.02 and (△) 0.1 ml, with the latter data taken 2 months after the former. The predictions of plate height and the break-up into its constituent contributions are as in Fig. 3. Note that an *ReSc* value of 20 corresponds to a velocity of about 1.0 cm/min.

less-steel column which was slurry-packed in our laboratory without any specialized equipment, the slight discrepancy between data sets acquired 2 months apart using different sample volumes was most likely caused by bed settling, leading to a small additional dispersion, rather than by loading effects. It should be noted that the plate heights for the 11.5-cm glass column do not uniformly exceed those from the 46.5-cm column even at low velocities (where the separation efficiency is highest and hence most susceptible to extraneous broadening). We also estimated the effect of the pair of headers on the broadening by using a liquid hold-up in each end-piece of 0.055 ml (as obtained from Omnifit) and by assuming each header to be a well-stirred tank (a single plate), as a worst-case limit; this contribution to the reduced plate height was found to be 0.006 for the short column. Hence the dispersion due to the headers is negligible and well within the scatter in the data.

The major ambiguity in the prediction of plate height concerns the estimates of convective dispersion made using Gunn's correlation and the Miller and King data. As seen from the figures, the two sets of predictions appear to bracket the data over most of the range of velocities. At the lower end of reduced velocities, where convective axial dispersion is the dominant contributor to the plate height, the

agreement between our data and the predictions based on the Miller and King fit is much better than that with the Gunn correlation. Note that, contrary to some claims [5], the dispersive contribution to reduced plate height resulting from mixing in the headers or extra-column hold-up is too small to explain the discrepancy between our low-velocity data and those of Hiby [23] (recall the discussion regarding Fig. 1). Hence the discrepancies between prediction and observation are not very large and would probably be of little consequence for design purposes: neither equilibrium nor transport parameters are likely to be known with sufficient accuracy in practice to allow such small distinctions to be made meaningfully.

It is then reasonable to state that for the systems investigated here, *a priori* prediction of the performance of well-packed columns *based on independent estimates of transport parameters* is, for almost all practical purposes, as good as direct measurement via chromatographic experiments. (It is important to reiterate that the *a priori* predictions mentioned here refer only to plate heights and not to equilibrium parameters such as inclusion porosities, an accurate determination of which is best left to measurement.)

This conclusion is important for several reasons. (1) It suggests that both the design of and the packing procedure for the columns used here were adequate to give maximum performance for the media considered, and that further design refinements are not essential for these types of separations, at least at low loadings. (2) It is not necessary, or indeed desirable, to go to the expense of obtaining monodisperse packings: there would be no significant gain in separation effectiveness by making such a change, and there is in fact reason to believe that a moderate degree of polydispersity may be helpful. It is well known, for example, that polydispersed particles give higher packing densities, and it appears that monodisperse packings can give rise to long-range wall effects [30,68]. The spherical symmetry of the particles, combined with the cylindrical symmetry of the wall, decreases the local packing density near the wall significantly, and the tendency towards long-range order in monodisperse packings can cause wall-induced irregularities to persist for long distances. Polydispersity, on the other hand, tends to break up such long-range effects. Moreover, as mentioned before, packings with a modest size distribution do not produce major increases in pressure drop over what is expected of their monodisperse counterparts for a given interstitial void fraction [59]. (3) These results suggest that simulation studies *based on accurate transport and equilibrium parameters* can be both useful and inexpensive for optimizing separations. Moreover, as both diffusivities and dispersion coefficients can usually be estimated fairly easily, it should be possible to guide the beginning stages of experimental investigations, thus obtaining attractive process specifications at a very early step in the process development. This consideration is particularly important for modern pharmaceutical production where process specifications tend to be frozen fairly early. (4) The success of simple transport models for predicting the behavior of chromatographic columns suggests the possibility of developing alternate types of contactors, such as true counterflow devices [69], on a rational basis.

Although the experiments described here were carried out on non-adsorptive systems, the above conclusions can be extended with some confidence to more complex situations. For example, the results on the effect of particle size distribution should also apply to adsorptive media, as the contribution to the plate height due to the finite rate of adsorption is independent of particle size. Finally, we feel that more work needs to be undertaken to characterize better the convective dispersion in packed beds for reduced velocities between 1 and 100 where there is an acute paucity of reliable information.

ACKNOWLEDGEMENTS

We gratefully acknowledge financial and material assistance from Rohm and Haas Company (Philadelphia, PA, USA). We appreciate the several valuable discussions with Drs. Edward Firouztale, Peter G. Cartier and Robert A. Albright of Rohm and Haas, and the help received from Dr. Michael Byers of TosoHaas who generously provided the packed glass columns. S.J.G. and E.N.L. thank the National Science Foundation for a Fellowship and for NSF Grant CBT-8901406, respectively. We also thank the State of Wisconsin for making possible the purchase of the Gilson apparatus used in this work.

SYMBOLS

A_0 column cross-sectional area (cm^2)
c_b volume-averaged solute concentration in a sorbent particle (mg/ml)
c_f solute concentration in moving fluid phase (mg/ml)
Da Damköhler number, defined as $R^2k_a/\mathscr{D}_p$
$\mathscr{D}_f$ effective solute diffusivity in unbounded solution (cm^2/s)
$\mathscr{D}_p$ effective solute diffusivity in pore liquid (cm^2/s)
$\mathscr{E}$ convective axial dispersion coefficient (cm^2/s)
$\mathscr{F}$ local sorption rate in the stationary phase (mg/ml·s)
H height equivalent to a theoretical plate (HETP) or plate height (cm)
h reduced plate height, $H/2R$
K_d ratio of masses of adsorbed and pore-liquid solutes at equilibrium
k_a (forward) rate constant of adsorption (s^{-1})
k_c concentration-based fluid-phase mass-transfer coefficient (cm/s)
m,m' parameters in the reduced plate height expression, defined in eqn. 7
m_0 mass of solute fed to column in a pulse (mg)
Nu fluid-phase Nusselt number, defined as $2Rk_c/\mathscr{D}_f$
$Pe_{\mathscr{E}}$ dispersion Péclet number, defined as $2Rv/\mathscr{E}$
p empirical parameter in Gunn's correlation, defined in eqn. 10
R radius of a stationary-phase particle (cm or μm)
r radial coordinate inside a spherical particle (cm or μm)
Re Reynolds number, defined as $2Rv\varepsilon_b\rho/\mu$
$ReSc$ reduced velocity or diffusion Péclet number, defined as $2Rv\varepsilon_b/\mathscr{D}_f$
Sc Schmidt number, defined as $\mu/\rho\mathscr{D}_f$
t time (s or min)
u fraction of solute in the moving fluid phase at long times, defined in eqn. 4
v interstitial fluid velocity, based on the area $\varepsilon_b A_0$ (cm/s or cm/min)
w_p concentration in pore liquid, based on unit volume of stationary phase (mg/ml)
w_s concentration of adsorbed solute, based on unit volume of stationary phase (mg/ml)
Y dimensionless group in Gunn's correlation, defined in eqn. 12
z axial coordinate in a packed bed (cm)
z_0 mean position of a solute peak at a given time, defined as uvt (cm)

GREEK LETTERS

α_1 smallest zero of the Bessel function $J_0(\cdot)$; *ca.* 2.405
β low $ReSc$ asymptote of the Nusselt number (eqn. 17)
γ parameter in the correlation for Nu (eqn. 16), defined as $1.09/\varepsilon_b$
ε_b interstitial (interparticle) void fraction in a packed bed
ε_p^* (intraparticle) inclusion porosity of a solute
μ fluid viscosity (g/cm·s)
ρ fluid density (g/cm^3)
τ bed tortuosity factor in Gunn's correlation; value 1.4

APPENDIX

Here we provide a formulation of the chromatographic equations to which the asymptotic solution has been presented in the section Chromatographic Model. The problem statement given below has been included in order to explain the notation used in this paper, which is different from that in the original source of this model [1].

The convective transport of solute by the mobile fluid phase in a granular bed is commonly described by a one-dimensional, pseudo-continuum model in which one neglects non-uniformities within the bed to write

$$\varepsilon_b\left(\frac{\partial c_f}{\partial t} + v\cdot\frac{\partial c_f}{\partial z} - \mathscr{E}\cdot\frac{\partial^2 c_f}{\partial z^2}\right) = -(1-\varepsilon_b)\frac{\partial c_b}{\partial t} \qquad \text{(A1)}$$

where c_f and c_b refer to the concentrations of a solute in the mobile and stationary phases, respectively, v is the interstitial velocity and ε_b is the interstitial void fraction of the bed (see Symbols). Here, we have assumed dispersed plug flow in the bed, with the convective axial dispersion coefficient $\mathscr{E}$ used to account for axial molecular diffusion and the hydrodynamic broadening effects associated with the local non-uniformities in the interstitial fluid velocity that

are caused by the complicated flow paths around sorbent particles. The use of a second-derivative (pseudo-Fickian) term to capture the effect of convective axial dispersion is justified for long, linear systems because the resulting Gaussian solution to a pulse input agrees well with observations on such systems.

The governing equations for solute transport inside a porous sorbent particle, assuming spherical symmetry and neglecting surface diffusion, are as follows:

$$\frac{\partial w_p}{\partial t} = \frac{\mathscr{D}_p}{r^2} \cdot \frac{\partial}{\partial r}\left(r^2 \cdot \frac{\partial w_p}{\partial r}\right) - \mathscr{F}(w_p, w_s) \qquad \text{for } 0 \leqslant r \leqslant R \tag{A2}$$

$$\frac{\partial w_s}{\partial t} = \mathscr{F}(w_p, w_s) \qquad \text{for } 0 \leqslant r \leqslant R \tag{A3}$$

$$\frac{\partial w_p}{\partial r} = 0 \qquad \text{for } r = 0 \tag{A4}$$

Here the local concentrations of solute present in the pore fluid (w_p) and adsorbed on the internal surfaces (w_s) are based on a unit volume of stationary phase (*i.e.*, the solid matrix and the pore space) rather than on the respective phase volumes within a particle. The assumption of linear adsorption kinetics allows us to express the local sorption rate $\mathscr{F}$ as

$$\mathscr{F}(w_p, w_s) = k_a\left(w_p - \frac{w_s}{K_d}\right) \tag{A5}$$

where k_a is the forward rate constant of adsorption, and the equilibrium constant K_d is simply the ratio of the mass of adsorbed solute to that of unadsorbed solute within a particle at equilibrium. The overall stationary-phase concentration of solute, c_b, is defined as

$$c_b \equiv (4\pi R^3/3)^{-1} \int_0^R (w_p + w_s) 4\pi r^2 dr \tag{A6}$$

The link between the mobile phase and stationary phase descriptions is provided by the matching condition of flux continuity at the particle surface:

$$-\mathscr{D}_p \cdot \frac{\partial w_p}{\partial r} = k_c\left(\frac{1}{\varepsilon_p^*} \cdot w_p - c_f\right) \quad \text{for } r = R \tag{A7}$$

where k_c is the fluid-phase mass-transfer coefficient. We distinguish here between the absolute intraparticle porosity of the stationary phase, which does not appear explicitly in our model, and the solute-dependent inclusion porosity (or an overall rejection factor) ε_p^* which, as seen from eqn. 4, gives the effective volume fraction of the stationary phase that is accessible to the solute. The advantage of using such an inclusion porosity is that we do not need to consider the intraparticle porosity and the rejection factor as separate geometrical parameters [5], which, in any event, are difficult to measure individually. This notation also couches the concentrations of the pore fluid and adsorbed solute, and thus the equilibrium distribution constant K_d, in experimentally meaningful and hence more practically useful terms.

The model formulation is now complete except for the initial and boundary conditions, which are discussed in the main text.

REFERENCES

1 S. J. Gibbs and E. N. Lightfoot, *Ind. Eng. Chem. Fundam.*, 25 (1986) 490–498.
2 J. C. Giddings, *Dynamics of Chromatography. Part I: Principles and Theory* (*Chromatographic Science Series*, Vol. 1), Marcel Dekker, New York, 1965.
3 D. M. Ruthven, *Principles of Adsorption and Adsorption Processes*, Wiley, New York, 1984.
4 J. Å. Jönsson in J. Å. Jönsson (Editor), *Chromatographic Theory and Basic Principles* (*Chromatographic Science Series*, Vol. 38), Marcel Dekker, New York, 1987, Ch. 2, pp. 27–102.
5 A. M. Lenhoff, *J. Chromatogr.*, 384 (1987) 285–299.
6 S. G. Weber and P. W. Carr, in P. R. Brown and R. A. Hartwick (Editors), *High Performance Liquid Chromatography* (Chemical Analysis Series, Vol. 98), Wiley, New York, 1989, Ch. 1, pp. 1–115.
7 J. J. van Deemter, F. J. Zuiderweg and A. Klinkenberg, *Chem. Eng. Sci.*, 5 (1956) 271–289.
8 L. Lapidus and N. R. Amundson, *J. Phys. Chem.*, 56 (1952) 984–988.
9 J. B. Rosen, *J. Chem. Phys.*, 20 (1952) 387–394.
10 A. Rasmuson, *AIChE J.*, 27 (1981) 1032–1035.
11 J. F. G. Reis, E. N. Lightfoot, P. T. Noble and A. S. Chiang, *Sep. Sci. Technol.*, 14 (1979) 367–394.
12 A. Klinkenberg and F. Sjenitzer, *Chem. Eng. Sci.*, 5 (1956) 258–270.
13 I. Stakgold, *Green's Functions and Boundary Value Problems*, Wiley, New York, 1979.
14 C. N. Satterfield, C. K. Colton and W. H. Pitcher, *AIChE J.*, 19 (1973) 628–635.
15 R. R. Walters, *J. Chromatogr.*, 249 (1982) 19–28.
16 B. F. D. Ghrist, M. A. Stadalius and L. R. Snyder, *J. Chromatogr.*, 387 (1987) 1–19.
17 R. B. Bird, W. E. Stewart and E. N. Lightfoot, *Transport Phenomena*, Wiley, New York, 1960.

18 M. F. Edwards and J. F. Richardson, *Chem. Eng. Sci.*, 23 (1968) 109–123.
19 D. J. Gunn and C. Pryce, *Trans. Inst. Chem. Eng.*, 47 (1969) T341–T350.
20 E. A. Ebach and R. R. White, *AIChE J.*, 4 (1958) 161–169.
21 G. L. Jacques, A. Hennico, J. S. Moon and T. Vermeulen, *Lawrence Radiation Lab. Rep.*, UCRL-1069, Part II, 1964.
22 S. F. Miller and C. J. King, *AIChE J.*, 12 (1966) 767–773.
23 J. W. Hiby, in A. Rottenburg (Editor), *Proceedings of Symposium on Interaction between Fluids and Particles*, Institution of Chemical Engineers, London, 1962, pp. 312–325.
24 D. J. Gunn, *Trans. Inst. Chem. Eng.*, 47 (1969) T351–T359.
25 C. L. De Ligny, *J. Chromatogr.*, 49 (1970) 393–401.
26 D. J. Gunn, *Chem. Eng. Sci.*, 42 (1987) 363–373.
27 J. R. Cluff and S. J. Hawkes, *J. Chromatogr. Sci.*, 14 (1976) 248–255.
28 N. W. Han, J. Bhakta and R. G. Carbonell, *AIChE J.*, 31 (1985) 277–288.
29 M. N. E. Rifai, W. J. Kaufman and D. K. Todd, *Sanitary Eng. Res. Lab. Rep.*, No. 3, IER Series 90, Berkeley, CA, 1956.
30 J. H. Knox and J. F. Parcher, *Anal. Chem.*, 41 (1969) 1599–1606.
31 S. F. Miller and C. J. King, *Lawrence Radiation Lab. Rep.*, UCRL-11951, 1965.
32 D. S. Horne, J. H. Knox and L. McLaren, *Sep. Sci.*, 1 (1966) 531–554.
33 S. Yamamoto, K. Nakanishi and R. Matsuno, *Ion-Exchange Chromatography of Proteins (Chromatographic Science Series*, Vol. 43), Marcel Dekker, New York, 1988, Ch. 5, pp. 161–170.
34 D. L. Koch and J. F. Brady, *J. Fluid Mech.*, 154 (1985) 399–427.
35 S. J. Gibbs, *Ph.D. Thesis*, University of Wisconsin–Madison, 1989.
36 W. E. Stewart, *AIChE J.*, 9 (1963) 528–535.
37 E. J. Wilson and C. J. Geankoplis, *Ind. Eng. Chem. Fundam.*, 5 (1966) 9–14.
38 H. Martin, *Chem. Eng. Sci.*, 33 (1978) 913–919.
39 J. P. Sørensen and W. E. Stewart, *Chem. Eng. Sci.*, 29 (1974) 811–837.
40 P. Fedkiw and J. Newman, *Chem. Eng. Sci.*, 33 (1978) 1043–1048.
41 D. J. Gunn and J. F. C. DeSouza, *Chem. Eng. Sci.*, 29 (1974) 1363–1371.
42 T. Miyauchi, T. Kikuchi and K.-H. Hsu, *Chem. Eng. Sci.*, 31 (1976) 493–498.
43 A. J. Karabelas, T. H. Wegner and T. J. Hanratty, *Chem. Eng. Sci.*, 26 (1971) 1581–1589.
44 J. H. Knox, *J. Chromatogr. Sci.*, 10 (1972) 549–556.
45 J. H. Knox, *J. Chromatogr. Sci.*, 15 (1977) 352–365.
46 J. H. Knox and H. P. Scott, *J. Chromatogr.*, 282 (1983) 297–313.
47 E. N. Lightfoot, S. J. Gibbs, A. M. Athalye and T. H. Scholten, *Isr. J. Chem.*, 30 (1990) 229–237.
48 K. Nakanishi, S. Yamamoto, R. Matsuno and T. Kamikubo, *Agric. Biol. Chem.*, 42 (1978) 1943–1945.
49 T. H. Scholten, *Ph.D. Thesis*, University of Wisconsin–Madison, Madison, WI, 1990.
50 J. V. Dawkins, T. Stone and G. Yeadon, *Polymer*, 18 (1977) 1179–1184.
51 A. S. Moharir, D. Kunzru and D. N. Saraf, *Chem. Eng. Sci.*, 35 (1980) 1795–1801.
52 A. S. Moharir, D. N. Saraf and D. Kunzru, *Chem. Eng. Commun.*, 11 (1981) 377–386.
53 A. Rasmuson, *Chem. Eng. Sci.*, 40 (1985) 621–629.
54 G. Carta and J. S. Bauer, *AIChE J.*, 36 (1990) 147–150.
55 Y. S. Lin and Y. H. Ma, *AIChE J.*, 36 (1990) 1569–1576.
56 D. O. Cooney, B. A. Adesanya and A. L. Hines, *Chem. Eng. Sci.*, 38 (1983) 1535–1541.
57 L.-I. Kulin, P. Flodin, T. Ellingsen and J. Ungelstad, *J. Chromatogr.*, 514 (1990) 1–9.
58 C. Dewaele and M. Verzele, *J. Chromatogr.*, 260 (1983) 13–21.
59 S. Yamamoto, M. Nomura and Y. Sano, *J. Chem. Eng. Jpn.*, 19 (1986) 227–231.
60 J. Germershausen, R. Bostedor, R. Liou and J. D. Karkas, *J. Chromatogr.*, 270 (1983) 383–386.
61 W. E. Stewart, M. Caracotsios and J. P. Sørensen, *Computational Modelling of Reactive Systems*, Butterworths, London, 1992, in preparation.
62 TosoHaas Technical Service Center, Woburn, MA, personal communication, 1990.
63 S. Yamamoto, M. Nomura and Y. Sano, *J. Chromatogr.*, 394 (1987) 363–367.
64 S. J. Gibbs, A. C. Chu, E. N. Lightfoot and T. W. Root, *J. Phys. Chem.*, 95 (1991) 467–471.
65 S. J. Gibbs, E. N. Lightfoot and T. W. Root, in preparation.
66 M. T. Tyn and T. W. Gusek, *Biotechnol. Bioeng.*, 35 (1990) 327–338.
67 C. R. Jones, C. S. Johnson and J. T. Penniston, *Biopolymers*, 17 (1978) 1581–1593.
68 R. C. Dean, presented at the *American Society of Mechanical Engineers Seminar on Process Equipment Technology for the Manufacture of Biopharmaceuticals, University of Virginia, September 26, 1989*, lecture 5.
69 E. N. Lightfoot, A. M. Athalye and D. K. Roper, in preparation.